Resistive type gas sensing and complex optical properties of *ex situ* Bi_2O_3 loaded polypyrrole

A. R. CHOUDHARY, S. A. WAGHULEY[a,*]
Department of Physics, Suresh Deshmukh College of Engineering, Wardha 442 001, India
[a]Department of Physics, Sant Gadge Baba Amravati University, Amravati 444 602, India

Present investigation describes simple chemical synthesis of Bi_2O_3 loaded polypyrrole (PPy) composites are prepared by ex-situ approach. As prepared composites show good sensing performance towards liquefied petroleum gas (LPG). The sensing response of composites has been observed good dependence on loading concentration of Bi_2O_3 in PPy. Main achievement of present work is that the operating temperature (353 K) of composite (25 wt %) is found much below the auto-ignition temperature of LPG. Besides that composites exhibit good complex optical properties such as extinction coefficient, optical conductivity, real and imaginary dielectric constant.

1. Introduction

Liquefied petroleum gas (LPG) is a versatile fuel generally used in industrial, commercial, agricultural, horticultural and manufacturing applications. But incorrect handling of LPG can result in explosions, fires and most importantly loss of lives. Therefore it is imperative that to take care of its leakage. Thus detection of LPG at low concentration is very much necessary. Intrinsically LPG has no smell and it is a colorless liquid that evaporates into a gas at room conditions. The artificial odorant is added to LPG for its primary detection. Hence in present work, we make an attempt to detect LPG at low concentration using Bi_2O_3 loaded polypyrrole (PPy) composites.

Some recent applications associated with PPy based materials are reviewed. Shinde et al [1] carried out novel and simple approach for synthesis of PPy thin film. The thin film deposited by chemical bath deposition has been used for supercapacitor application. Geng et al [2] has been synthesized hybrid material polypyrrole/Fe_2O_3 by using sol–gel polymerization technique. Results of this study shows that content of $Fe(NO_3)_3.9H_2O$ in PPy increase the uniformity of molecular weight of PPy. Hybrid material PPy/Fe_2O_3 has been exhibited good sensitivity towards NH_3 at considerably low operating temperature (<100 °C). Mi et al [3] has been reported synthesis of PPy nanotubes by using complex of methyl orange (MO)/$FeCl_3$ as a template. The in-situ approach has been adopted for preparation of core–shell polypyrrole/polyaniline (PPy/PANI) composite. Electrochemical characterization of PPy/PANI composite resulted that composite has significant specific capacitance 416 F g^{-1} in 1M H_2SO_4 electrolyte with good rate capability. Yang et al [4] has been described nanofibers of PPy using simple reactive template ($FeCl_3$ and methyl orange) approach. Concluding remarks of this study

suggested that large scale production of PPy nanofibers is possible with said technique. The comparative gas sensing study of bulk and nanofibers PPy shows that PPy nanofibers have been exhibited significantly superior performances. Sharma et al [5] synthesized PPy by in-situ electrosynthesized approach on gold electrode by using four different scan rate variations. As-prepared PPy electrode has been used to study electrochemical behavior of nerve agents stimulant that is dimethyl methyl phosphonate (DMMP) in aqueous medium. Carquigny et al [6] did the fabrication of micro-gas-sensors based on poly(pyrrole) thin films as sensing layer. Result of this study reflected that electrical response of sensors has been influenced by temperature and concentration. The comparative study between most of resistive sensors indicates that PPy-based sensor has been improved sensing response, selectivity, stability and reproducibility.

Su et al [7] fabricated flexible NH_3 gas sensors on plastic substrates by in situ self-assembly of PPy. The sensing response and flexibility of sensors were optimized towards NH_3 gas. The comparative response between flexible and rigid substrate at room temperature demonstrated that flexible NH_3 gas sensor exhibits a strong response.

Pirsa et al [8] has been reported detection of pyridine derivatives by using gas sensor based on nanostructure conducting PPy. Sensing behavior of PPy gas sensor showed rapid detection of pyridine derivatives. The result of this study confirmed that determination of pyridine derivatives from cigarette smoke is possible by using fabricated sensor.

Patois et al [9] synthesized PPy by chemical polymerization for detection of ammonia. Prepared sensor specified good sensing response for lower concentration in the range 1ppm-100 ppm with high sensitivity at room temperature. Rawal et al [10] have synthesized chemically

nanostructure PPy in presence of anionic azo dye and cationic surfactant. As-synthesized both samples have different shapes and dimensions. The surface area of PPy synthesized in the presence of anionic azo dye has higher surface area compared to cationic surfactant. Concluding remark of this study intensively observed that PPy nanowires have higher sensitivity towards PPy nanoparticles. Joshi et al [11] have synthesized PPy thin films by in-situ chemical polymerization. As-synthesized PPy thin film used to fabricate gas sensor and its gas sensing performance tested towards NH_3 and NO at room temperature. PPy thin film based gas sensor showed good selectivity towards NH_3 and the sensitivity in range of 4–80 ppm. Temmer et al [12] reported the novel approach of combined chemical–electrochemical synthesis of PPy-based actuators. PPy based actuator was yielded with good reproducible, functional actuators with acceptable displacement. Li et al [13] fabricated nanocomposite based on SnO_2 nanosheets and PPy. Prepared nanocomposites have been tested towards NH_3 and investigated at room temperature. Nanocomposite based sensor shows 6.2%/ppm sensitivity towards NH_3 with detection limit of ~257 ppb. Sun et al [14] adopted microemulsion polymerization technique for synthesize PPy/Au nanocomposites. As-prepared nanocomposite particles have tetrahedron structure. The excellent electrical conductivity obtained for PPy/Au nanocomposites of the order of 12.6± 0.06 S/cm. Li et al [15] synthesized nano-scaled PPy particles by using Triton X-100 micelles via soft template approach. Prepared PPy nanoparticles spin coated on surface acoustic wave transducers to sense acetone gas. In 5.5 ppm to 80 ppm concentration range, response of sensor was linear and sensor has fast response and recovery times of 9 s and 8.3 s, respectively.

Ni et al prepared graphene oxide decorated silver nanoparticles electrode by an amperometry method. Pyrrole monomer was electropolymerized on surface of modified electrode through amperometry technique. The result of this study indicated that first linear section was in the range of 0.1–5 mM with a limit of detection of 1.099 [16]. Chougule et al [17] have been prepared PPy/zinc oxide nanocomposite by using spin coating method. As-synthesized nanocomposite tested towards the CH_3OH, C_2H_5OH, NH_3, H_2S and NO_2 at room temperature. The nanocomposite represents the excellent gas sensing properties towards NO_2 at concentration as low as 10 ppm with 92.10% stability to 100 ppm NO_2 gas at room temperature.

Navale et al [18] prepared PPy/α-Fe_2O_3 hybrid nanocomposite on glass substrate by spin coating technique. Sensing response of nanocomposite revealed that as-prepared detects NO_2 at low concentration (10ppm) with very high selectivity (18%) and sensitivity (56%) with better stability. Zou et al [19] prepared core-shell composite consisting of PPy nanofibers as core and TiO_2 as shell. As prepared core-shell composite further doped with Pd nanoparticles via chemical reduction. As fabricated Pd–TiO_2@PPy-based sensor exhibited a sensitivity of 8.1% toward 1vol% of H_2 gas. An et al [20] prepared composite between PPy/carbon aerogel by using

chemical oxidation polymerization through ultrasound irradiation. This result showed that composite material has a high specific capacitance of 433 F g^{-1}.

In present communication, we successfully prepared ex-situ Bi_2O_3 loaded PPy composites by simple chemical route. Screen printing technique is used to fabricate the resistive type gas sensors in the form of thick films. Prepared composite materials are characterized by using XRD, Raman spectroscopy, SEM and TG-DTA. The sensors exposed to LPG at room temperature and sensing response measured is noted in term of change in electrical resistance of sensors. The sensing behavior of ex-situ Bi_2O_3 loaded PPy composites discussed using adsorption mechanism. By considering outstanding optical properties of hybrid materials, we also planned to investigate the complex optical parameters of Bi_2O_3 loaded PPy composites. In the present work, complex optical parameters like optical band gap, extinction coefficient, optical conductivity, real dielectric constant and imaginary dielectric constant were studied.

2. Experimental

In this work, AR grade SD fine, India chemicals were used for preparation of Bi_2O_3 loaded PPy composites. The procured chemicals were used without any purification. Chemical oxidative route method was used to synthesize PPy. The ex-situ approach was adopted for preparation of composites. In this approach, concentration of Bi_2O_3 nanoparticles alter from 5 wt.%-25 wt.% with an interval of 5 wt.% by keeping PPy concentration constant. Both constituents of composite were mixed in organic media to obtain good homogenous composite. In this way, different five samples of composite were obtained for preparation of gas sensors. The classical screen printing method was used to fabricate gas sensor. Thick film of as-prepared materials deposited on chemically clean glass substrate. Ohmic contact of conducting electrode (silver) was deposited on both sides of film. Description of gas sensor assembly is mentioned in our previous report [21]. XRD pattern of composites was recorded on Rigaku Miniflex-II, X-ray diffractometer. The surface morphology of sample was examined by using scanning electron microscope (SEM) JEOL JSM-7500F. Thermal properties of composite were analyzed by using Shimadzu DTG-60h. The Raman spectroscopic data for composites was acquired using Bruker RFS 27 Raman spectrometer. UV-VIS spectrum of sample was recorded on Agilent Cary 60 spectrophotometer.

3. Results and discussion

Fig. 1 displays the XRD pattern of ex-situ Bi_2O_3 loaded (a) 5 wt.%, (b) 10 wt.%, (c) 15 wt.%, (d) 20 wt.% and (e) 25 wt.% in PPy. Minute analysis of XRD pattern of composites showed that composites samples have semi-crystalline nature. Some sharp peaks on broad hump appeared in the range $2\theta=30^o-36^\circ$ [22]. The diffraction

pattern indicates that ultra-small clusters of Bi$_2$O$_3$ nanoparticles were present on granular surface of PPy, which was responsible for the semi-crystalline nature of composites. The intensity of diffraction peak at 35.1° increased with doping concentration of Bi$_2$O$_3$ in PPy. This indicated that degree of crystallinity improved with concentration of Bi$_2$O$_3$ in PPy. The 25 wt.% of Bi$_2$O$_3$ loaded PPy has highest peak intensity.
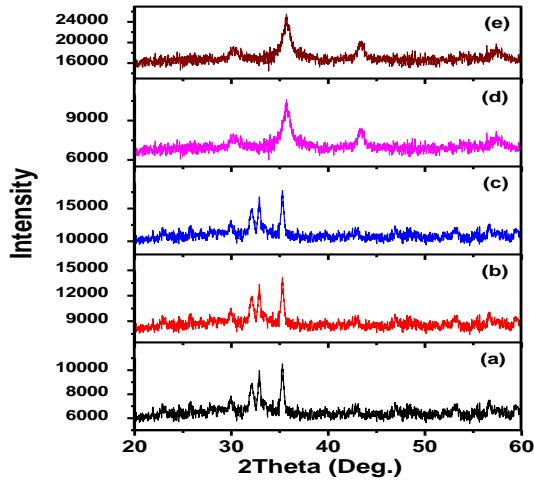
Fig. 1. XRD pattern of different composites samples prepared by altering wt.% concentration of Bi$_2$O$_3$ (a) 5 wt.%, (b) 10 wt.%, (c) 15 wt.%, (d) 20 wt.% and (e) 25 wt.% in PPy.

Average polymer chain separation is mainly affected by synthesis conditions and concentration of dopant. Similarly average polymer chain separation has direct effect on electrical conductivity. Therefore electrical conductivity has crucial role in gas sensing study. Average chain separation values for Bi$_2$O$_3$ loaded PPy samples were computed using equation (Eq. 1),

$$R = \left| \frac{5\lambda}{8Sin\theta} \right| \qquad (1)$$

where R is polymer chain separation in Å, λ is X-ray wavelength (1.541 Å) and θ is diffraction angle at high intensity amorphous halo. The calculated value of average chain separation for composite samples is listed in Table 1.

Table 1. Average chain separation value and particle size of different composite samples prepared by altering wt.% concentration of Bi$_2$O$_3$ (a) 5 wt.%, (b) 10 wt.%, (c) 15 wt.%, (d) 20 wt.% and (e) 25 wt.% in PPy.

Sample	Peak position of amorphous halo (θ) °	Average chain separation (Å)	Particle size (nm)
5 wt.%	17.60	1.014	16.71
10 wt.%	17.68	1.045	16.72
15 wt.%	17.60	1.014	16.71
20 wt.%	17.82	1.123	16.73
25 wt.%	17.75	1.080	16.72

Morphology of composites was characterized by using SEM images. Fig. 2 represents SEM images of ex-situ Bi$_2$O$_3$ (a) 5 wt.%, (b) 10 wt.%, (c) 15 wt.%, (d) 20 wt.% and (e) 25 wt.% loaded PPy composites. Bi$_2$O$_3$ loaded PPy composites exhibited irregular morphology, which might be attributed to the formation of PPy layer formed by polymerization process. No substantial difference in morphology of composites was observed. The blurry boundaries of composites indicate semi-crystalline nature. The Bi$_2$O$_3$ nanoparticles were not observed in composite, it indicates that Bi$_2$O$_3$ is being nicely enwrapped by PPy. The irregular morphology is generally preferred than uniform morphology for gas sensor fabrication, due to large adsorption of gas molecules on irregular morphology [23, 24].
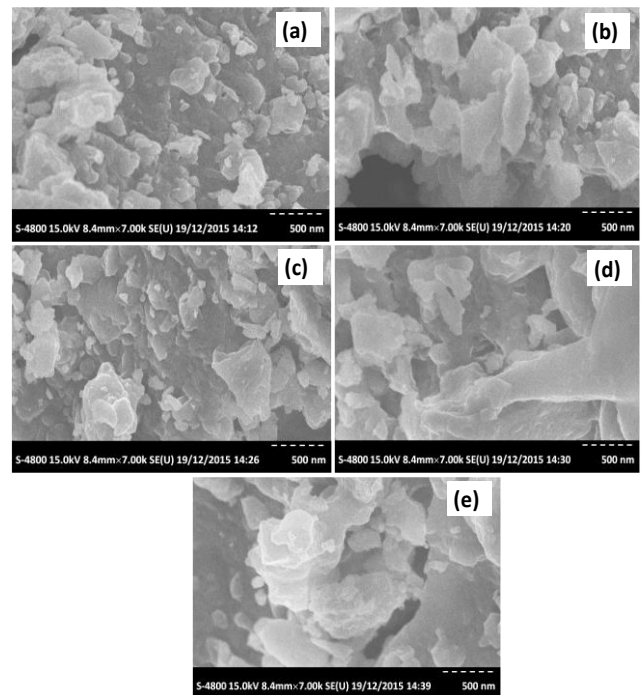
Fig. 2. SEM images of different composite samples prepared by altering wt.% concentration of Bi$_2$O$_3$ (a) 5 wt.%, (b) 10 wt.%, (c) 15 wt.%, (d) 20 wt.% and (e) 25 wt.% in PPy.

In order to analyze structural aspect of composites and understanding of doping state, Raman spectroscopy was performed. Fig. 3 shows the Raman spectrum of ex-situ Bi$_2$O$_3$ loaded (a) 5 wt.%, (b) 10 wt.%, (c) 15 wt.%, (d) 20 wt.% and (e) 25 wt.% in PPy composites. The bands appear in higher frequency side around 1517 and 1581 cm^{-1}, which is attributed to vibration band and C=C stretching band of PPy in composite samples. Weak band at 1590 cm^{-1} and 1605 cm^{-1} is assigned to overlapping of cationic and dicationic bands in highly oxidized polymer, respectively [25, 26]. The decrease of oxidation level was observed from shifting band toward lower frequency side. The oxidized ring deformation and C-H in-plane bending in composite sample confirmed from two bands ~1420 and 1330 cm^{-1}, respectively [27]. The band at 988 and

$1050 \ cm^{-1}$ ascribed to ring deformation and C-H in plane bending band [28].
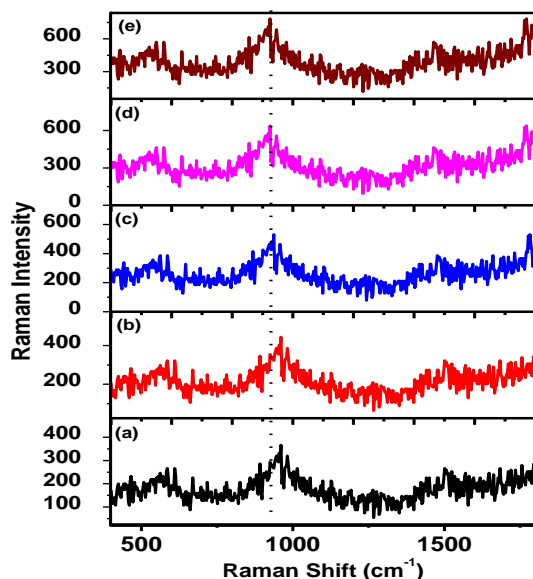
Fig. 3. Raman pattern composites samples prepared by altering wt.% concentration of Bi_2O_3 (a) 5 wt.%, (b) 10 wt.%, (c) 15 wt.%, (d) 20 wt.% and (e) 25 wt.% in PPy

Fig. 4 depicts the variation of % TGA and DTA curves of 25 wt.% Bi_2O_3 loaded PPy composite as function of temperature. Continuous mass loss was observed up to 475 K. The first step of mass loss up to 373 K is attributed to removal of moisture and constituted water. Beyond 373 K, carboneous gas released from composite which significantly reduced the mass of composite. The major peak at 370 K attributed to phase change.
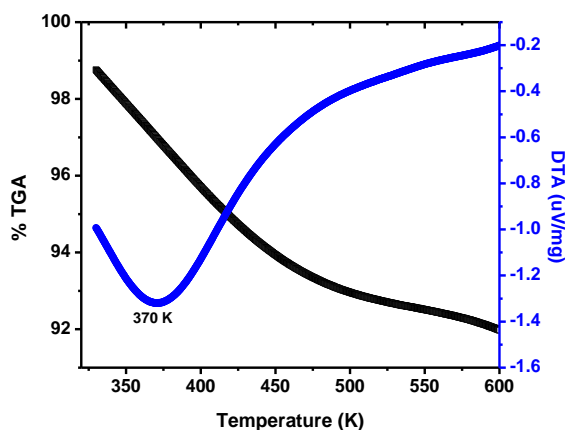
Fig. 4. TG-DTA of 25 wt.% Bi_2O_3 loaded PPy composite

Fig. 5 depicts selectivity response of Bi_2O_3 loaded (a) 5 wt.%-S1, (b) 10 wt.%-S2, (c) 15 wt.%-S3, (d) 20 wt.%-S4 and (e) 25 wt.%-S5 in PPy. In present work, selectivity response was tested towards 25 ppm LPG and CO_2 gas concentration at room temperature. The selectivity of

sensor is nothing but the ability of sensor to sense a particular gas with high sensitivity at fixed concentration and temperature. In Fig. 5, Bi_2O_3 loaded PPy composites shows higher sensitivity towards the LPG than CO_2 gas. This indicates that as-prepared composites were more selective towards the LPG.
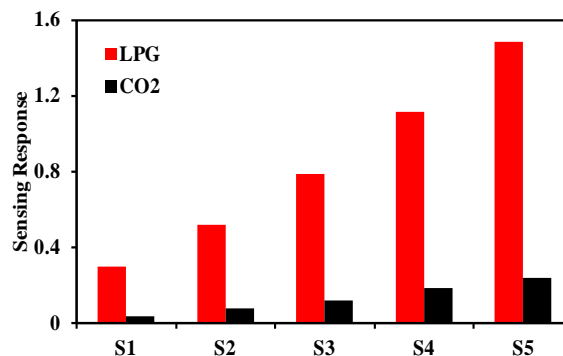
Fig. 5. Selectivity response of Bi_2O_3 loaded (a) 5 wt.%-S1, (b) 10 wt.%-S2, (c) 15 wt.%-S3, (d) 20 wt.%-S4 and (e) 25 wt.%-S5 in PPy composites

Fig. 6 shows the sensing response of Bi_2O_3 loaded (a) 5 wt.%-S1, (b) 10 wt.%-S2, (c) 15 wt.%-S3, (d) 20 wt.%-S4 and (e) 25 wt.%-S5 in PPy composites. In this work, sensing response is measured in terms of change in resistance. The sensing response was measured at room temperature as a function of varying concentration. The plot exhibits that sensors shows good dependence on concentration of LPG up to 50 ppm. In this response curves, most of sensors shows linearity up to 35 ppm. The 25 wt.% Bi_2O_3 loaded PPy composite has highest sensing response. From the plot, it is observed that sensing response increase with loading concentration of Bi_2O_3 in PPy. This enhancement in sensing response might be due to two reasons, first is addition of Bi_2O_3 in PPy creates free electrons in composites and another is increasing presence of Bi_2O_3 in PPy responsible for adsorption of more numbers of oxygen molecules on the sensing surface [29, 30].
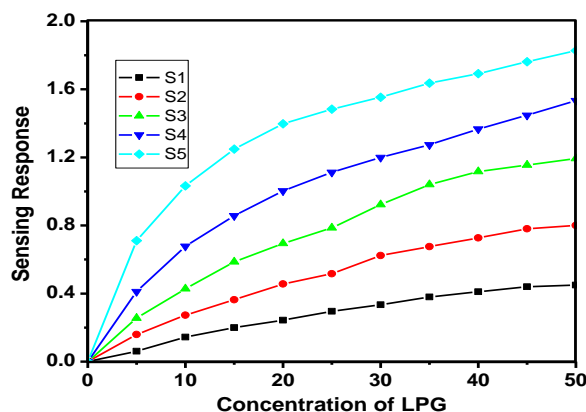
Fig. 6. Gas sensing response of different Bi_2O_3 loaded PPy composite samples towards the LPG at room temperature

It is well known that in gas sensing process adsorbed oxygen molecules play very crucial role. Generally, reaction for adsorption of oxygen on gas sensing surface is represented by (Eq.(2)-(4)) [31],

$$O_2 \text{ (gas)} \rightarrow O_2 \text{ (ads)} \tag{2}$$

$$O_2 \text{ (ads)} + e^- \rightarrow O_2^- \text{ (ads)} \tag{3}$$

$$O_2^- \text{ (ads)} + e^- \rightarrow 2O^- \text{ (ads)} \tag{4}$$
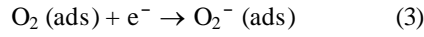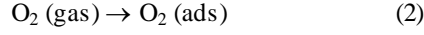
The exchange of electrons between sensing surface and target is happened through these adsorbed oxygens. In our case, target gas is LPG, which is composition of CH_4, C_3H_8, C_4H_{10} etc. All these listed gases have strong tendency to add electrons to sensing surface, due to reducing nature of LPG.

The reaction between composition of LPG and adsorbed oxygen are presented as follows (Eq.(5), (6)) [32].

$$C_nH_{2n+2} + 2O^- \text{ (ads)} \rightarrow H_2O + C_nH_{2n}{:}\,O + e^- \tag{5}$$

$$C_nH_{2n}{:}\,O + O^- \text{ (ads)} \rightarrow CO_2 + H_2O + e^- \tag{6}$$
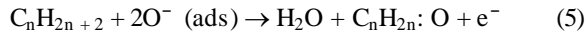
Thus in present case, addition of Bi_2O_3 in PPy increases density of adsorbed oxygen on composite surface, which results in addition of more number of electrons in conduction band of composites. Therefore resistance of composite decrease and which is reflected from the enhancement of sensing response. Therefore, 25 wt.% Bi_2O_3 loaded PPy composite has higher response towards the LPG.

Fig. 7 shows operating temperature response of 25 wt.% Bi_2O_3 loaded PPy composite. The operating temperature response of composite was tested for fixed value of 25 ppm LPG as a function of varying temperature. From Fig. 7, it is observed that up to particular value of temperature sensing response increases and then starts to decrease. This temperature point at which sensing response achieves highest value is known as operating temperature of sensor. In our case, 25 wt.% Bi_2O_3 loaded PPy composite has operating temperature value 353 K. Beyond operating temperature, sensing response decrease because internal thermal vibration transfers to adsorbed oxygen. Thus at higher temperature oxygen is desorbed from sensing surface. This results in decrease of sensing response. The operating temperature value of sensor is much below auto-ignition temperature of LPG. This is main accomplishment of present work with Bi_2O_3-PPy composite.
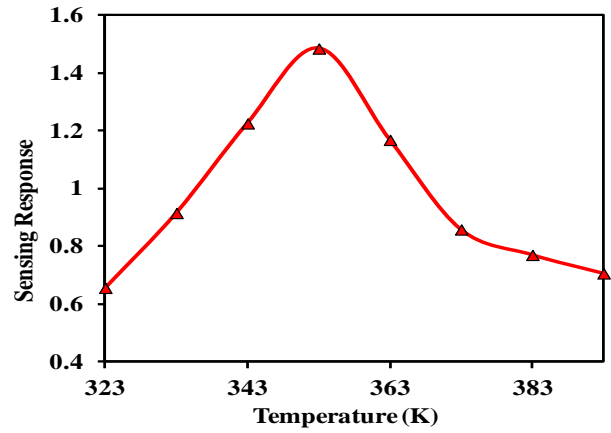
Fig. 7. Operating temperature performance of 25 wt.% Bi₂O₃ loaded PPy sample towards the 25 ppm LPG

The response and recovery characteristics of 25 wt.% Bi_2O_3 loaded PPy composite is shown in Fig. 8. The response and recovery characteristic of sensor was tested towards 25 ppm concentration of LPG at room temperature (303 K). Plot shows that sensor has rapid response towards the target gas. The sensor achieved highest value of sensing response to LPG in 30 s. As compared to response time, recovery time was slow. This may be due to the chemisorbed target molecules not readily dissociate from sensing surface [33]. Thus sensor required more time to achieve its original value in air. The recovery time for sensor was more than 50 s.
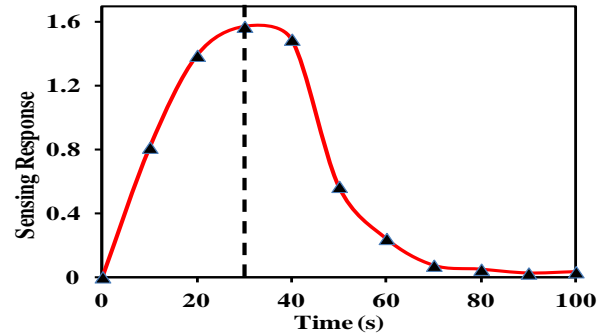
Fig. 8. Response and recovery performance of 25 wt.% Bi₂O₃ loaded PPy sample towards the 25 ppm LPG

Fig. 9 depicts stability response of 25 wt.% Bi_2O_3 loaded PPy sample against LPG at room temperature (303 K). The stability response was collected against 25 ppm LPG for a month. Stability response was collected by an interval of 5 days. No significant deviation in response observed for entire month. This indicates that as-fabricated sensor is stable for practical applications [34].
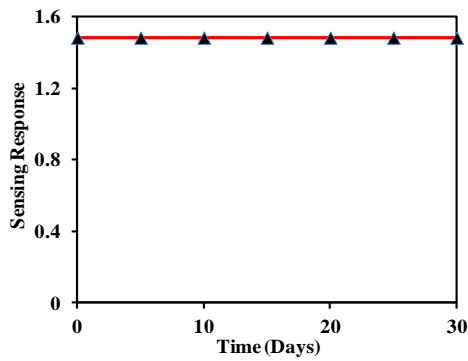
Fig. 9. Stability performance of 25 wt.% Bi_2O_3 loaded PPy sample towards the 25 ppm LPG

Fig. 10 shows the UV-VIS spectra of Bi_2O_3 loaded (a) 5 wt.%-S1, (b) 10 wt.%-S2, (c) 15 wt.%-S3, (d) 20 wt.%-S4 and (e) 25 wt.%-S5 in PPy composites. From figure 10, it is directly observed that absorption tail of composite shifted towards longer wavelength with addition of Bi_2O_3 in PPy composites. By extrapolating straight line to the UV-VIS curves on wavelength axis band gap composites was determined. The wavelength-energy relation was used to compute band gap of composites. The band gap shows decrease in value with addition of Bi_2O_3 in PPy composites. The possible reason for decrease in band gap that is red shift is may be due to increase in particle size. In materials science, it is very well known that band gap and particle size are inversely related. In our case, sample shows red shift in other words decreases in band gap. It indicates that with addition of Bi_2O_3, average particle size of composite increases through agglomeration process. The rate of agglomeration for organic materials in the presence of finer crystals is high. Therefore average particle size composite was increases with Bi_2O_3 concentration in composites.
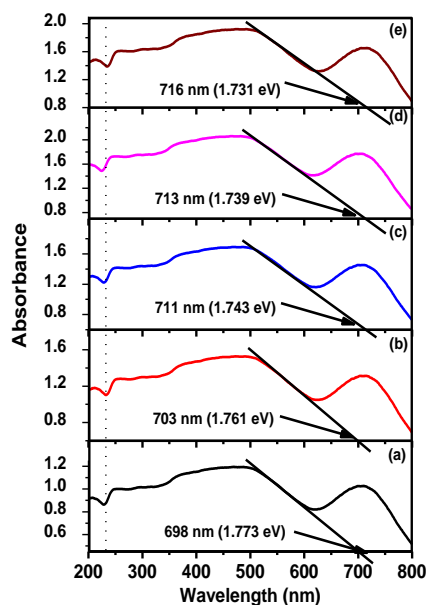
Fig. 10. UV-VIS spectra of samples prepared by altering wt.% concentration of Bi_2O_3 (a) 5 wt.%, (b) 10 wt.%, (c) 15 wt.%, (d) 20 wt.% and (e) 25 wt.% in PPy.

Fig. 11 depicts variation of extinction coefficient with wavelength. Plot shows that extinction coefficient nearly same between 200-225 nm. Beyond it extinction coefficient linearly increases up to 500 nm. The extinction coefficient shows highest value around 712 nm. It indicates that as-prepared composites have highest ability to trap light in visible region up to 712 nm. The sample with composition 20 wt.% Bi_2O_3 loaded PPy composite has highest value of extinction coefficient. The extinction coefficient is indicator of ability to restrict the light [35]. The 20 wt.% Bi_2O_3 loaded PPy composite possesses highest ability to restrict light, it may be due to good polymeric network supported by inorganic materials exist in composites.
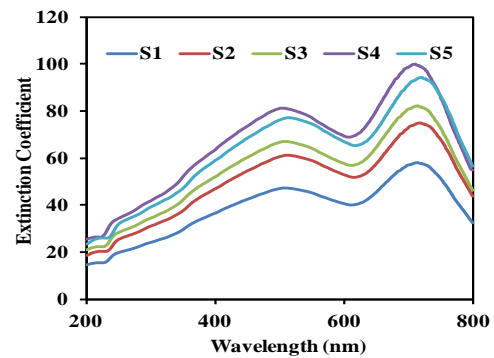
Fig. 11. Variation of Extinction coefficient of samples prepared by altering wt.% concentration of Bi_2O_3 (a) 5 wt.%, (b) 10 wt.%, (c) 15 wt.%, (d) 20 wt.% and (e) 25 wt.% in PPy.

Fig. 12 shows influence of Bi_2O_3 concentration in PPy on optical conductivity of as-prepared composites. Fig. 12 show that optical conductivity has good dependence on concentration of Bi_2O_3 concentration in PPy composite. Optical conductivity values determined by using relation Eq. (7) [36],

$$\sigma = \frac{\alpha c n}{4\pi} \qquad (7)$$

where α is absorption, c is velocity of light and n is refractive index. The value of refractive index is estimated by using the relation Eq. (8),

$$n = \frac{1}{\%T} + \sqrt{\frac{1}{\%T} - 1} \qquad (8)$$

where %T is transmission composite sample under investigation. As expected, higher value of optical conductivity was found to be for 20 wt.% Bi_2O_3 loaded PPy composites. In all composite samples, optical conductivity value is higher in wavelength range 225-500 nm. This variation of optical conductivity curve indicates that free charge carriers are constantly produced between 225-500 nm.
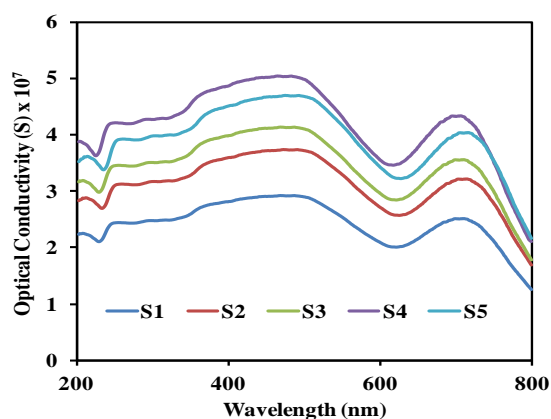
Fig. 12. Variation of optical conductivity of samples prepared by altering wt.% concentration of Bi₂O₃ (a) 5 wt.%, (b) 10 wt.%, (c) 15 wt.%, (d) 20 wt.% and (e) 25 wt.% in PPy.

Fig. 13 (a) and (b) shows variation of real and imaginary dielectric constant of Bi₂O₃ loaded (a) 5 wt.%-S1, (b) 10 wt.%-S2, (c) 15 wt.%-S3, (d) 20 wt.%-S4 and (e) 25 wt.%-S5 in PPy composites. Dielectric constant is complex function which has two parts real and imaginary dielectric constant. Physics point of view both parts have different physical interpretation. The real dielectric constant of materials shows the ability of material to slow down the light. Therefore it depends on the refractive index of materials. While, imaginary dielectric constant is used to represent degree of interaction among electric field and dipole present in medium. In our case, both parts have same variation with wavelength but magnitude is different. This shows that in as-prepared samples the degree of interaction between an electric field and dipole is lower than the light slow down ability. The 20 wt.% Bi₂O₃ loaded PPy composite has highest degree of interaction between an electric field and dipole [37].
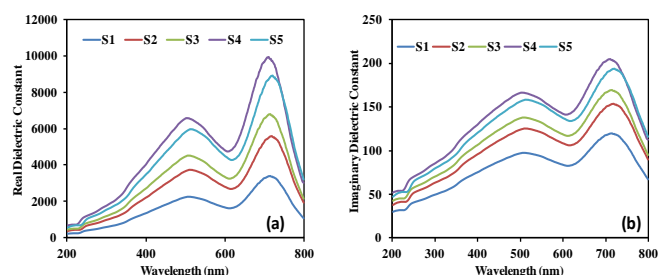
Fig. 13. Variation of (a) real and (b) imaginary dielectric constant of samples prepared by altering wt.% concentration of Bi₂O₃ (a) 5 wt.%, (b) 10 wt.%, (c) 15 wt.%, (d) 20 wt.% and (e) 25 wt.% in PPy.

4. Conclusions

The Bi₂O₃ loaded PPy composite was prepared by simple chemical route in ex-situ format. Using classical screen printing method, gas sensors were fabricated and demonstrated for sensing application. As prepared composite materials reveals good selectivity and high sensing magnitude towards the target gas that is LPG. Composite samples were more selective towards reducing gas. As LPG detection is more important at low concentration, we analyzed sensing response of composite material up to 50 ppm only. The highest sensing response was observed for the 25 wt.% Bi₂O₃ loaded PPy composite. This may be due to sensing surface adsorbed oxygen species which is responsible for change in resistance due to Bridging oxygens. The reducing gas like LPG added electrons through adsorbed oxygen to sensing surface. Therefore resistance of materials was found to be decrease significantly in presence of LPG gas due to its reducing nature. Operating temperature for composite was found to be 353 K for 25 ppm concentration of LPG. The rapid response and recovery time witnessed for 25 wt.% Bi₂O₃ loaded PPy composite. The 25 wt.% Bi₂O₃ loaded PPy composite based sensor shows good stability against 25 ppm concentration of LPG at room temperature for 30 days. The complex optical parameters of Bi₂O₃ loaded PPy composite were evaluated for varying concentration of Bi₂O₃ in PPy. Optical properties of composites were seems to be strappingly affected by the concentration of Bi₂O₃ in PPy. Optical band gap of sample decreases with increasing concentration of Bi₂O₃. The 20 wt.% Bi₂O₃ loaded PPy composites shows good complex optical properties such as extinction coefficient, optical conductivity, real and imaginary dielectric constant. This study shows that Bi₂O₃ loaded PPy composite may be employed for opto-electronics applications.

References

[1] S. S. Shinde, G. S. Gund, V. S. Kumbhar, B. H. Patil, C. D. Lokhande, E. Polym. J. **49**(11), 3734 (2013).
[2] L. Geng, S. Wu, Mater. Res. Bull. **48**(10), 4339 (2013).
[3] H. Mi, X. Zhang, X. Ye, S. Yang, J. Power Sour. **176**(1), 403 (2008).
[4] X. Yang, L. Li, Synth. Met. **160**(11-12), 1365 (2010).
[5] P. K. Sharma, G. Gupta, V. V. Singh, B. K. Tripathi, P. Pandey, M. Boopathi, B. Singh, R. Vijayaraghavan, Synthetic Met. **160**(23-24), 2631 (2010).
[6] S. Carquigny, J. Sanchez, F. Berger, B. Lakard, F. Lallemand, Talanta **78**(1), 199 (2009).
[7] P. Su, C. Lee, C. Chou, Talanta **80**(2), 763 (2009).
[8] S. Pirsa, N. Alizadeh, Talanta **87**, 249 (2011)
[9] T. Patois, J. Sanchez, F. Berger, P. Fievet, O. Segut, V. Moutarlier, M. Bouvet, B. Lakard, Talanta **117**, 45 (2013).
[10] I. Rawal, A. Kaur, Sens. Actuators A **203**, 92 (2013).

[11] A. Joshi, S. A. Gangal, S. K. Gupta, Sens. Actuators B **156**(2), 938 (2011).

[12] R. Temmer, I. Must, F. Kaasik, A. Aabloo, T. Tamm, Sens. Actuators B **166**, 411 (2012).

[13] Y. Li, H. Ban, M. Yang, Sens. Actuators B **224**, 449 (2016).

[14] L. Sun, Y. Shi, B. Li, L. Chu, Z. He, J. Liu, Colloids and Surf. A: Physicochem. Eng. Aspects **397**, 8 (2012).

[15] F. Li, H. Li, H. Jiang, K. Zhang, K. Chang, S. Jia, W. Jiang, Y. Shang, W. Lu, S. Deng, M. Chen, App. Surf. Sci. **280**, 212 (2013).

[16] P. M. Ni, F. Lorestani, W. P. Meng, Y. Alias, App. Surf. Sci. **332**, 648 (2015).

[17] M. A. Chougule, D. S. Dalavi, Sawanta Mali, P. S. Patil, A. V. Moholkar, G. L. Agawane, J. H. Kim, Shashwati Sen, V. B. Patil, Measurement **45**(8), 1989 (2012).

[18] S. T. Navale, G. D. Khuspe, M. A. Chougule, V. B. Patiln, Ceramics Int. **40**(6), 8013 (2014).

[19] Y. Zou, Q. Wang, D. Jiang, C. Xiang, H. Chu, S. Qiu, H. Zhang, F. Xu, L. Sun, S. Liu, Ceramics Int. **42**(7), 8257 (2016).

[20] H. An, Ying Wang, Xianyou Wang, Liping Zheng, Xingyan Wang, Lanhua Yi, Li Bai, Xiaoyan Zhang, J. Power Sour. **195**(19), 6964 (2010).

[21] K. R. Nemade, S. A. Waghuley, J. Electronic Materials **42**(10), 2857 (2013).

[22] A. Kassim, H. N. M. E. Mahmud, L. M. Yee, N. Hanipah, Pac. J. Sci. Technol. **7**(2), 103 (2006).

[23] J. Xu, Q. Pan, Y. Shun, Z. Tian, Sens. Actuators B **66**(1-3), 277 (2000).

[24] H. J. Kharat, K. P. Kakade, P. A. Savale, K. Dutta, P. Ghosh, M. D. Shirsat, Polym. Adv. Technol. **18**(5), 397 (2007).

[25] K. Crowley, J. Cassidy, J. Electroanal. Chem. **547**(1), 75 (2003).

[26] F. Chen, G. Shi, M. Fu, L. Qu, X. Hang, Synth. Met. **132**(2), 125 (2003).

[27] K. Crowley, J. Cassidy, J. Electroanal. Chem. **547**(1), 75 (2003).

[28] J. Arjomandi, A. U. Shah, S. Bilal, H. V. Hoang, R. Holze, Spectrochim. Acta, Part A **78**, 1 (2011).

[29] K. R. Nemade, S. A. Waghuley, Journal of Mater. Sci. and Engineering **B 3**, 310 (2013).

[30] K. R. Nemade, S. A. Waghuley, Int. J. Chem. Tech. Res. **6**(6), 3399 (2013).

[31] K. R. Nemade, S. A. Waghuley, Rare Metals **34**(1), 6 (2015).

[32] K. R. Nemade, S. A. Waghuley, St. Petersburg Polytechnical University Journal: Physics and Mathematics **1**(3), 249 (2015).

[33] K. R. Nemade, S. A. Waghuley, Journal of Mater. Sci. and Engineering **2**(1), 63 (2014).

[34] K. R. Nemade, S. A. Waghuley, Applied Nanoscience **5**(4), 419 (2015).

[35] K. R. Nemade, S. A. Waghuley, Int. J. Metals **2014**, 389416 (2014).

[36] N. A. Bakr, A. M. Funde, V. S. Waman, M. M. Kamble, R. R. Hawaldar, D. P. Amalnerkar, S. W. Gosavi, S. R. Jadkar, Pramana **76**, 519 (2011).

[37] R. V. Barde, K. R. Nemade, S. A. Waghuley, Optical Materials **40**, 118 (2015).

*Corresponding author: sandeepwaghuley@sgbau.ac.in